PRAMANA
—journal of
physics

© Printed in India

Vol. 49, No. 5,
November 1997
pp. 521–533

SCORPION: A system for coincidences between recoil and projectile ions at NSC, New Delhi

M J SINGH, S K GOEL, R SHANKER, D O KATARIA*, N MADHAVAN*, P SUGATHAN*, J J DAS*, D K AVASTHI* and A K SINHA*
Atomic Physics Laboratory, Department of Physics, Banaras Hindu University, Varanasi 221 005, India
*Nuclear Science Centre, P.O. Box 10502, New Delhi 110 067, India
email: rshanker@banaras.ernet.in

MS received 7 December 1996; revised 1 July 1997

Abstract. An on-line facility to measure coincidences between the recoil ions and the scattered projectiles (SCORPION) has been designed, fabricated and commissioned at Nuclear Science Centre (NSC), New Delhi. The facility consists of a four jaw slit assembly, a time of flight (TOF) spectrometer, a parallel plate electrostatic charge analyser and a one dimensional position sensitive parallel plate avalanche counter (PPAC). Details of the design and working principles of various components and the test results obtained for the Si^{q+}–Ar collision system are presented to highlight the performance of the system. A multiple loss of up to four electrons has been observed for 60 MeV Si^{4+} ions colliding with argon atoms in a single collision condition. Spectra of recoil ions detected in coincidence with a particular charge state of the scattered projectile show a bell shaped distribution as a function of the recoil charge state (r) for the electron loss events. However, the yield of recoil ions drops as r increases for the direct ionization channel. Also for electron loss, the peak of the recoil ion distribution is seen to shift to a higher recoil charge state as the number of lost electrons from the projectile increases.

Keywords. Coincidence technique; recoil ions; time of flight spectrometer.

PACS Nos 07.75; 34.50

1. Introduction

Coincidence measurements between the scattered projectile ions and the recoil ions have attracted the attention of many workers [1–4] since the inception of the field by Cocke [5]. These measurements help in understanding the multielectron processes which occur during the collisions of the type

$$A^{q+} + B \rightarrow A^{(q-i)+} + B^{p+} + (p-i)e^{-}. \tag{1}$$

Such studies not only provide an indepth information on the various fundamental processes (direct ionization, e^{-}-capture and e^{-}-loss) responsible for the production of multiply ionized recoil ions but also help in the understanding of the dynamics of such collisions. The scattered projectile ions $[A^{(q-i)+}]$ in the exit channel of the process described by eq. (1) have a mixture of charge states because of the finite probability of the occurrence of all the fundamental processes mentioned above. For the direct ionization case, $i = 0$, i.e. the charge state of the scattered projectile is identical to that of the incident one. For the electron capture case, $i > 0$ implying thereby that the charge state of the scattered projectile is less as compared to the charge state of the incident projectile depending on the number of electrons it has captured from the target atom during collision. For the electron loss case, $i < 0$, incident-ion loses additional electrons. Recently, a similar attempt in this direction has been pursued at the 15 UD Pelletron accelerator facility of Nuclear Science Centre (NSC) [6], New Delhi. Some measurements using a time-of-flight spectrometer (TOF) have been performed earlier, the details of which are presented elsewhere [7]. In these measurements the selection of the final charge state of the scattered projectile was not possible. As mentioned above, the separation of the various charge states of the scattered projectile is important to identify the channels leading to the recoil ion distributions for the various ionization processes. This can be achieved either by magnetic deflection [2, 4, 8] or by using a parallel plate electrostatic charge analyser [1, 3, 9]. A new facility, SCORPION (System for COincidences between the Recoil and Projectile IONs), which uses a parallel plate electrostatic charge analyser, has been developed and set up at the zero degree exit port of the general purpose scattering chamber (GPSC) [10] beam line of NSC. The set up has been used to perform coincidence measurements between the recoil ions and the charge selected scattered projectiles. This paper reports on the various hardware components of the SCORPION and their design details. A few typical results obtained from the data on Si^{q+}–Ar collisions using the SCORPION facility are presented and discussed.

2. Hardware details of SCORPION

The SCORPION set up for performing experiments on recoil ion projectile ion coincidences is shown in figure 1. The charge state of the recoil ions produced as a result of the interaction in a crossed beam geometry between the highly charged energetic ions

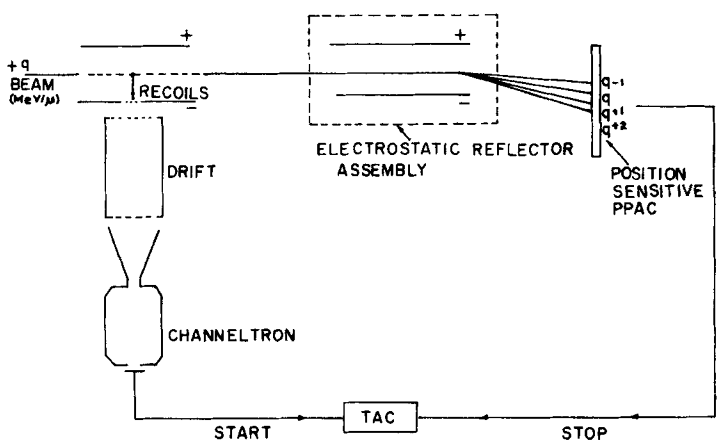

Figure 1. Schematic diagram of the set up for coincidences between recoils and projectile-ions.

with the neutral target atoms are separated using a TOF set up. The scattered projectiles moving in the forward direction are charge state separated by an electrostatic charge analyser and are finally detected by a one-dimensional position sensitive parallel plate avalanche counter (PPAC). The fine control of the incident beam is facilitated by a four jaw slit assembly. A brief description of the design and working principles of various components of the SCORPION set up is given below.

2.1 *Four jaw slit assembly*

The four jaw slit assembly connected to the exit port of the GPSC is an important part of the SCORPION set up. It is required for controlling the incident number of charged particles because of the limited count rate handling capabilities of the PPAC ($\sim 10^{4-5}$ particles/sec). It also helps in reducing the diameter of the incident beam which is helpful in optimizing the time resolution of the recoil ion peaks as will be highlighted in § 2.2. The assembly is an octagonal aluminum block of thickness 100 mm, in the centre of which a hole of 85 mm diameter is bored. The four orthogonal edges of this block are provided with a Wilson seal arrangement through which stainless steel (SS) shafts pass. The movement of the shafts is controlled with the help of micrometers. The rotational motion of the central shaft of the micrometer is converted into a linear motion of the SS shaft with the help of ball bearings. In order to lock even fine rotations of the shaft during its linear motion, proper guides have been provided. Four SS strips, bolted on the teflon pieces which are push fit at the ends of the shafts, form an aperture, the size of which can be varied with the help of micrometers. In overlapping position, the distance between any two strips is 2 mm. Each strip is connected to a hermetically sealed lemo connector for providing a current read out. The slit arrangement is followed by a bellow (internal diameter (ID) $\sim$ 100 mm) and a cross (ID $\sim$ 100 mm). This combination houses a Faraday cup for the GPSC.

The exit port of the cross is connected to an SS scattering chamber through a gate valve. The chamber supported by a stand has an internal diameter of 300 mm and a height of 150 mm. The TOF spectrometer is mounted in the chamber on the bottom port using an adapter. The mounting arrangement has the facility of height adjustment of the spectrometer together with the possibility of its rotation and translation in a direction perpendicular to the beam direction. These features help in proper alignment of the spectrometer with respect to the incoming beam direction. One of the ports of the scattering chamber has a gas handling flange with appropriate mountings.

2.2 *Time of flight spectrometer*

The TOF set up separates the recoils of various charge states on the basis of their time of flight over a certain path length. The set up consists of a pusher and an extractor plate (+ and −), a drift tube and a channeltron detector as shown in figure 1.

2.2.1 *Time resolution of the TOF spectrometer*: The advantage of such a spectrometer is its speed of collection of ions and a simple design, without any limitation on its shape and size. However, it is found to have a limited time resolution [11]. Ideally if all the recoil ions formed in the interaction zone have zero initial velocity and move parallel to the extraction field, then the time of flight of all the ions having the same mass to charge ratio will be the same and in this case the resolution of the spectrometer will be limited by the resolution of the detector. In practice, the other limiting factors contributing to the time spread are:

2.2.1.1 *Initial space distribution of ions*: Due to a finite width of the beam and the finite spread of the gaseous target atoms, ions are born at different positions. This leads to a variation in flight times of ions having the same m/q ratio.

2.2.1.2 *Initial kinetic energy distribution of ions*: The time spread due to an initial kinetic energy distribution of the ions is due to the difference in flight times of two ions born at the same position but with the velocity vectors pointing in opposite directions.

2.2.2 *Estimation of time spreads*: If the ions are born with an initial energy U_0, then the total energy of the ions in charge state q impinging on the detector (see figure 1) is given by

$$U = U_0 + qsE_s + qdE_d + qxE_x \tag{2}$$

where E_s, E_d and E_x are the electric fields in the spaces s, d and x respectively. The total time of flight is given by the relation

$$T = T_s + T_d + T_D + T_x \tag{3}$$

where,

T_D = time of flight throught drift length D,

$$T_s = \frac{(2m)^{1/2}}{qE_s}[(U_0 + qsE_s)^{1/2} - U_0^{1/2}], \tag{4}$$

$$T_d = \frac{(2m)^{1/2}}{qE_d}[(U_0 + qsE_s + qdE_d)^{1/2} - (U_0 + qsE_s)^{1/2}], \tag{5}$$

$$T_D = \frac{(2m)^{1/2}D}{2(U_0 + qsE_s + qdE_d)^{1/2}}, \tag{6}$$

$$T_x = \frac{(2m)^{1/2}}{qE_x}[(U)^{1/2} - (U_0 + qsE_s + qdE_d)^{1/2}]. \tag{7}$$

As mentioned in § 2.2.1.1, the time resolution of the spectrometer is limited by the time spread due to initial space distribution of ions. To minimise this time spread, it is necessary that all the ions having the same m/q and born around the mean s_0 reach the detector at the same time. The condition is satisfied if, at the detector

$$\left(\frac{dT}{ds}\right)_{U_0 s_0} = 0. \tag{8}$$

Using condition (8) in (3) and assuming that the ions are born with zero initial velocity, we get

$$D = 2(sE_s + dE_d)^{3/2}\left[\left(\frac{1}{sE_s}\right)^{1/2}\left(\frac{1}{E_s} - \frac{1}{E_d}\right) + \left(\frac{1}{sE_s + dE_d}\right)^{1/2}\left(\frac{1}{E_d} - \frac{1}{E_x}\right) + \left(\frac{1}{sE_s + dE_d + xE_x}\right)^{1/2}\left(\frac{1}{E_x}\right)\right], \tag{9}$$

where D gives the optimum drift length required for the best time resolution. To estimate the contribution from the time spread due to kinetic energy distribution (§ 2.2.1.2), consider two ions (ion 1 and ion 2) born at the same initial position s with the same initial speed but with their velocity vectors pointed towards + and − respectively. Ion 1 moves a certain length towards + before it is pulled back by the potential on −. Subsequently its motion is identical to that of ion 2 moving towards − from the beginning. Hence, the time difference between ion 1 and ion 2 reaching the detector is the 'turn around time' given by the relation,

$$T = \text{Turn around time} = 2\,(\text{Deceleration time}) = 2\frac{(2mU_0)^{1/2}}{qE_s}. \tag{10}$$

2.2.3 *Mass resolution*: The maximum resolvable mass, M, [11] depends on the initial space and energy distribution functions. Consider the relation

$$\frac{1}{M} = \frac{1}{M_s} + \frac{1}{M_\theta}, \tag{11}$$

where M_s is the maximum resolvable mass for which time spread due to space distribution of ions ΔT_s equals the time spread between adjacent mass peaks and M_θ is the maximum resolvable mass for which the time spread due to kinetic energy distribution of ions ΔT_θ equals the time between adjacent mass peaks. M will be smaller than either M_s or M_θ. On the other hand, it will be at least as large as the value M obtained above by assuming the total spread to be the sum of the energy and space time spreads.

2.2.4 *The present TOF spectrometer*: The TOF spectrometer is a SS box of dimensions 100 mm × 60 mm × 100 mm. The spectrometer, besides housing the TOF set up, has provisions for

(1) adjustable collimators for beam entrance and exit made from tantalum.
(2) arrangement for gas input through a hypodermic needle (diameter = 1 mm) with a provision for adjusting its height with respect to the incoming beam. The needle is connected to the gas handling flange through a nalgene tube of diameter 10 mm. The gas flow in the interaction region is controlled with the help of fine needle valves.

+ and − are copper plates of dimensions 20 mm by 20 mm and thickness 4 mm. The plates are separated from each other by 20 mm (= $2s$) with the help of teflon spacers. The extractor plate has a 5 mm circular hole in the centre for allowing the recoils to pass through after extraction from the interaction region. To avoid field penetration through the hole and through the ends of the drift tube, a grid of parallel wires (25 micron diameter wires spaced 1 mm apart) is epoxied using a conducting glue. The transmission efficiency of the grid is about 90%. The 30 mm (= D) long drift tube is separated from the extractor plate by 3 mm (= d). Following the drift tube is the channeltron detector spaced 5 mm (= x) from the end of the former.

2.3 *Parallel plate electrostatic charge deflector*

An ion of mass m, having an energy T and a charge state q suffers a deflection X when it passes through a pair of plates across which an electric field of E (kV/cm) exists. The deflection X is given by the expression

$$X = \frac{qeE}{4T}[L(L+2d)], \tag{12}$$

where L is the length of the deflector plate and d is the separation between the end of the deflector plate and the detector for the ions.

Using the above principle, a parallel plate electrostatic charge analyser set up was fabricated and mounted at the exit port of the scattering chamber. The assembly consists of two parallel aluminum plates, each 400 mm long and 60 mm wide. The plates are housed in a 150 mm O.D. and 600 mm long beam pipe. High voltage is applied to the plates through the specially designed feedthru's which are detachable. The feedthru is insulated from the beam pipe using teflon cylinders which pass through a Wilson seal arrangement provided in the housing for the plates. The length of the trapped air column between the feedthru and the teflon cylinder is reduced using a single O-ring which is pressed onto the plate by the cylinder. Such an arrangement reduces the chances of breakdown because of poor vacuum due to trapped gases. The place of application of high voltage is covered by a teflon cap. The gap between the plates can be varied with the help of nylon spacers. In the present arrangement, the plates are separated by 25 mm with the top plate being 5 mm above the beam height. The parallel plate deflector is followed by a bellow, a long tube, a TEE, a gatevalve and a PPAC. The total flight path of the ions after exiting from the charge analyser to the PPAC is 1600 mm, which is sufficient to provide a good separation between the charge states of the scattered projectile. The bellow helps in bending the entire assembly in such a way that for a given electric field between the plates, the incident charge state hits the centre of the detector with the charge states due to electron capture and loss on either side. The expected deflection of a 60 MeV Si^{4+} ion for a field of 1.2 kV/mm between the plates, as found out using (12) is 29 mm and the separation between neighbouring charge states is 7 mm.

The SCORPION incorporates pumping stations which are fitted with turbomolecular pumps to provide a oil-free vacuum.

2.4 *One dimensional position sensitive PPAC*

A one dimensional position sensitive PPAC [12] detector, mounted at the end of the SCORPION, is housed in a SS flange of diameter 100 mm. The window foil of the detector is a 1.6 μm aluminized mylar foil. The anode is a similar foil glued to 1.6 mm thick PCB. The cathode is a printed circuit board having aluminized parallel strips. The width of each strip is 1.4 mm and the spacing between the strips is 0.6 mm. The cathode is made position sensitive using the resistive chain method.

The value of the resistance between any two strips is 300 Ω. The spacing between two electrodes is 5 mm. The anode is kept at a high voltage whereas the two ends of the cathode are grounded through 100 MΩ resistances. The active area of the PPAC is 30 mm × 70 mm.

3. Commissioning tests of SCORPION

The entire assembly was pumped to a vacuum of 4×10^{-6} mbar. The GPSC, pumped by a 2000 l/sec diffstak pump showed a vacuum of 1×10^{-6} mbar. For initial tests, the PPAC was replaced by a glass viewport with quartz pieces stuck along the vertical central axis. With the slits fully open, a beam of 60 MeV Si^{4+} ions was allowed to fall onto alumina pieces stuck to the sides of the entrance collimator of the TOF spectrometer. The beam was focussed and steered so as to pass through the tantalum collimator. With a suitable electric field applied to the deflector plates, the bent beam was viewed on the quartz pieces of the glass ports. With changes in the voltages applied to the plates, the movement of the beam on the quartz pieces was observed. The tests ensured correct alignment of all the components of the SCORPION set up. The slits were closed using the micrometers and the decrease in the intensity of the spot was observed as expected.

3.1 *Coincidence measurements between recoils and scattered projectiles*

For the coincidence measurements, the view port at the end of the assembly was removed and replaced by the PPAC. Initially, the gate valve isolating the PPAC from the rest of SCORPION line was closed and the slits were fully opened. A pulsed, 60 MeV Si^{4+} beam from the accelerator, with a repetition rate of 1 μs, was properly focussed and passed through the spectrometer so as to crossfire a neutral beam of argon atoms. The flow of the gas was controlled with the help of the needle valves. The recoils in various charge state were extracted from the interaction region and made to drift towards the channeltron detector by using optimized voltages on the different components of the set up, which are listed in table 1. The signals from the channeltron were fed into a fast, current sensitive preamplifier. The TOF spectrum of the recoils was obtained by giving the 'start' signal to the time-to-amplitude converter (TAC) from the channeltron and a 'stop' signal from the rate divided RF. Single collision conditions

Table 1. Optimized values of voltages and distances in the time of flight set up.

Distance of the interaction region from − (s)	10 mm
Distance of the drift tube from − (d)	3 mm
Length of the drift tube (D)	30 mm
Distance of CEM from the drift tube (x)	5 mm
Voltage on + plate	+1 kV
Voltage on − plate	−1 kV
Voltage on the drift tube	−1.3 kV
Voltage on the channeltron	−2.2 kV

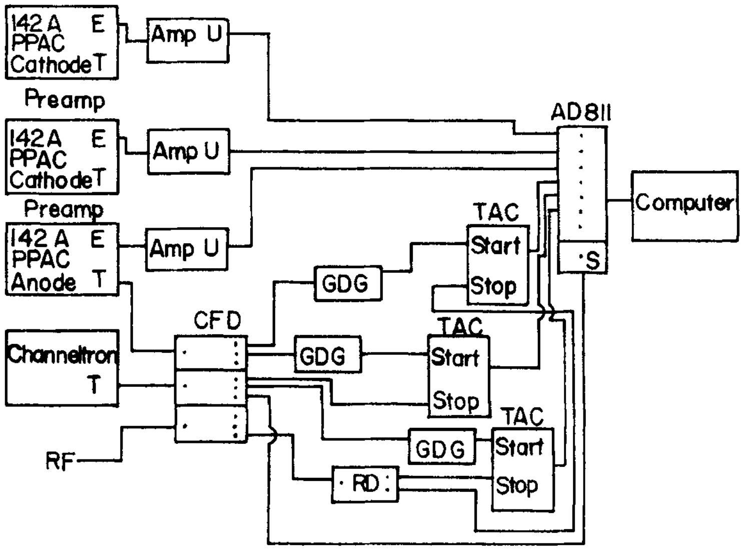

Figure 2. Schematic diagram of the electronics used to process the signals for the SCORPION experiment.

were ascertained by studying the variation in the yield of Ar^+ recoil ions normalized to the number of ions detected by the PPAC as a function of the gas pressure. In the absence of a capacitance manometer, the pressures were measured at the gas entrance with the help of a Pirani gauge and just below the TOF spectrometer with the help of a Penning gauge. After ensuring that single collision conditions prevailed in the interaction region, fine tuning of the beam was done to get an optimized argon recoil spectrum. The observed count rate of the channeltron was about 3000 counts per second. Following this the slits on the four jaw assembly were closed in a controlled fashion with the TOF spectrum being monitored after each change. Maintaining a consistent recoil-ion spectrum, the count rate in the channeltron was reduced from 3000 counts per second to 10 counts per second. Subsequently, voltages of ± 10 kV were applied to the deflector plates and the gate valve isolating the PPAC from the rest of assembly was opened. Slits were fine tuned so that the PPAC counted at a rate of 8 kHz to 10 kHz.

The electronic block diagram for processing the signals from the channeltron, the PPAC anode and the two ends of the PPAC cathode is shown in figure 2. The processed signals were fed to an analog to digital converter (ADC). A data acquisition program NSCSORT, is used to acquire the data in list mode. The strobe to the ADC was obtained from the channeltron. A typical TOF spectrum of the recoils produced in 60 MeV Si^{4+}–Ar collisions recorded from the channeltron–PPAC TAC is shown in figure 3 without any gating from the charge selected projectiles. The position spectrum of the charge separated projectiles shown in figure 4 for the 60 MeV Si^{4+}–Ar case was obtained by dividing the energy signal from one end of the cathode with the sum of the signals from both the ends. In addition to the incident beam charge state, projectiles which have lost up to 4 electrons are also seen. With the change in voltage of ± 2 kV on the deflector plates, the change expected in the position of the projectile peaks is ~ 4 mm. A

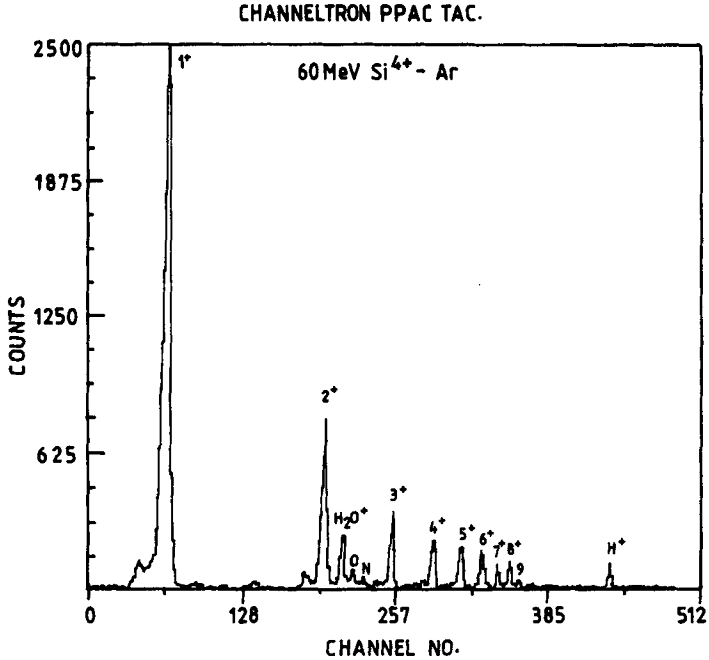

Figure 3. Time-of-flight spectrum of recoils obtained from the channeltron-PPAC-TAC for 60 MeV Si^{4+} ions interacting with argon gas.

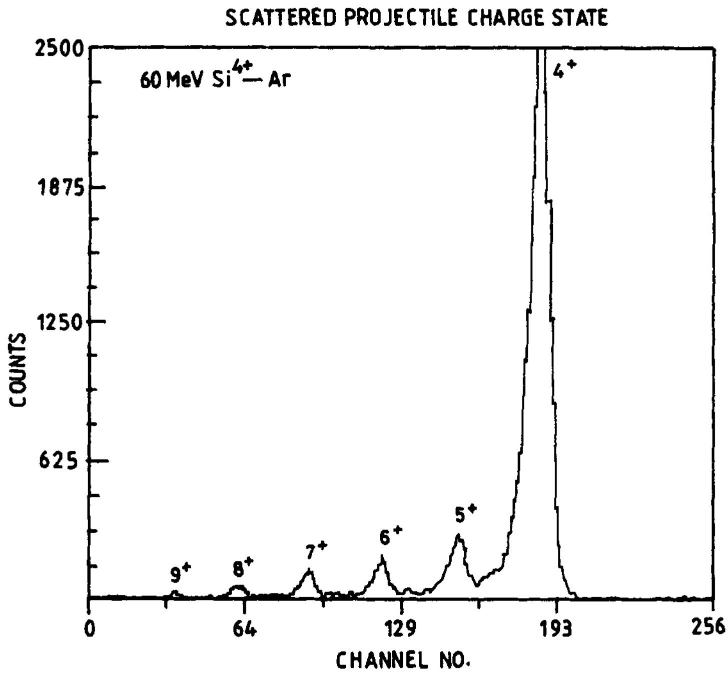

Figure 4. Position spectrum of the scattered projectiles produced in 60 MeV Si^{4+}–Ar collisions.

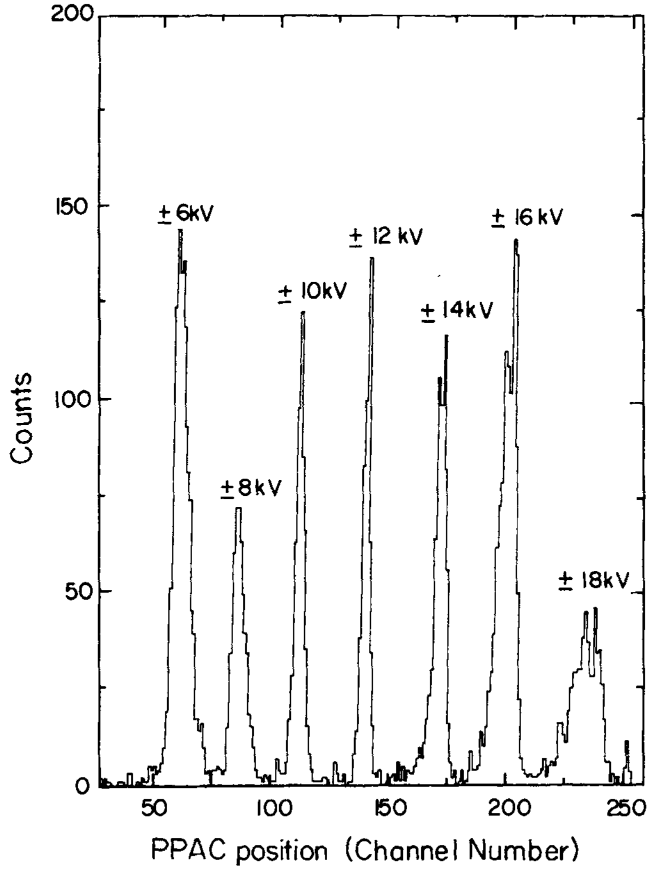

Figure 5. Position spectrum of the 60 MeV Si^{4+} charge state of the beam for the increase in the deflector plate voltage in steps of ± 2 kV.

typical position spectrum of the 60 MeV Si^{4+} charge state of the beam, for the variation in the voltages on the deflector plates in steps of ± 2 kV, is shown in figure 5. It may be noted that the time of aquisition is not the same for all the peaks. The channel numbers along the X axis correspond to the position of the PPAC in the vertical direction along which the deflection is observed.

4. Recoil ion distributions for various ionization channels

The recorded data were processed using the NSCSORT program in order to extract recoil ion spectra corresponding to particular charge states of the projectiles. With conditions applied to the total recoil-ion spectrum, the recoil ion distributions for direct ionization and for electron loss up to 4 electrons were obtained as shown in figures 6(a–e). For the direct ionization process (figure 6a), the recoil ion yield drops with the increase in the recoil charge state, indicating collisions with large impact parameters. The recoil ion distributions become bell shaped for the case of electron loss (figure 6b–e), with the peak of the distribution shifting to higher recoil charge states. This bell shaped distributions point to collisions of smaller impact parameters as compared to the direct ionization. The shifting of the peak to the higher recoil charge state with the increasing number of electrons lost by the incident ion indicates a deeper penetration by the projectile [3]. Note that for Si^{4+} incident beam, electron capture processes are not observed. On increasing the charge state of the incoming beam, the position spectrum of the scattered projectiles shows peaks which correspond to electron capture processes in addition to direct ionization and electron loss processes. Detailed results on the studies of direct ionization, electron capture and electron loss processes and their effect on the recoil ion distributions for 60–120 MeV Si^{q+}–Ar collision system will be reported elsewhere in a separate publication.

5. Conclusion

A facility to perform coincidences between recoil ions produced in fast, heavy, ion-atom collisions with the charge separated projectiles, has been developed and installed at NSC, New Delhi. The design features of the various components have been described in detail. This facility has been used to study the direct ionization, electron capture and electron loss channels in collisions of multiply charged silicon ions with neutral argon atoms. Some typical spectra of the recoil ions for various channels have been presented and briefly discussed.

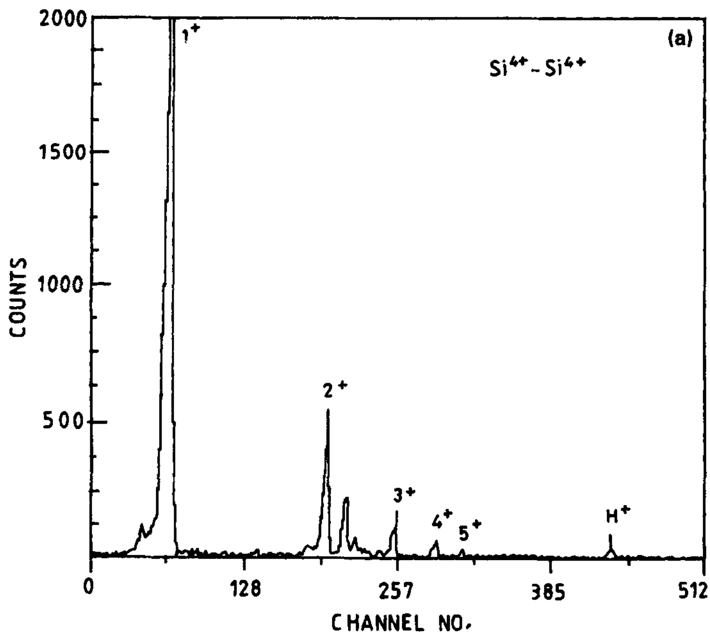

Figure 6(a).

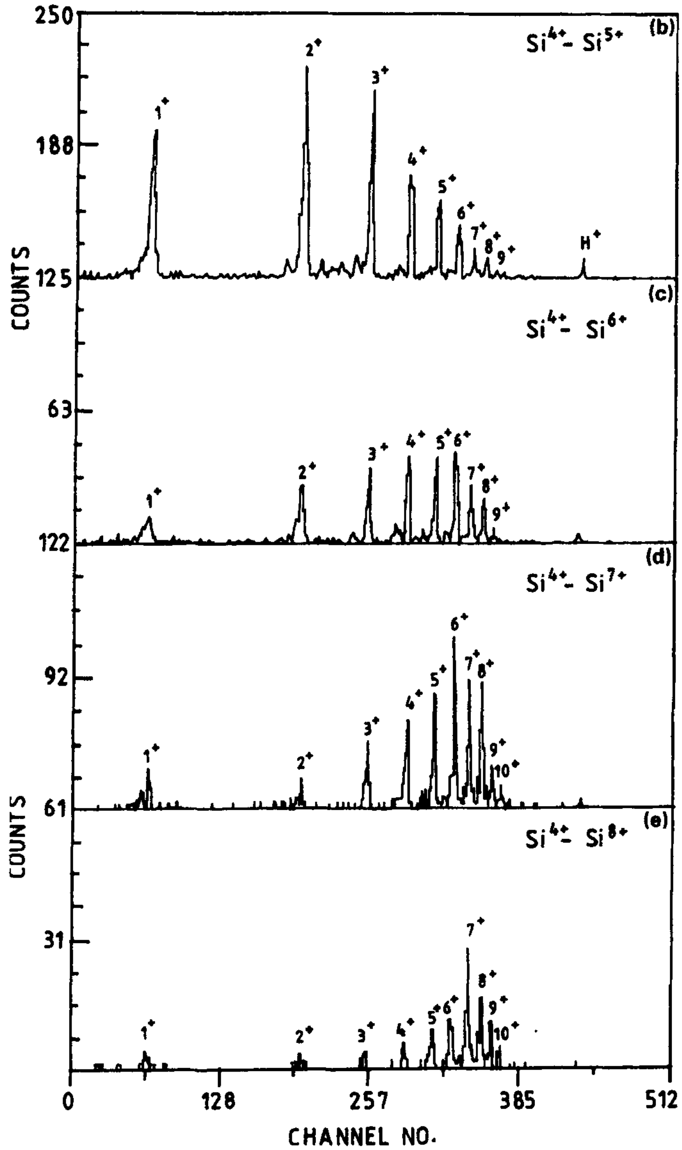

Figure 6. Recoil distributions corresponding to (**a**) direct ionization, (**b**) 1-e^- loss, (**c**) 2-e^- loss, (**d**) 3-e^- loss and (**e**) 4-e^- loss events in the case of 60 MeV Si^{4+}–Ar collisions.

Acknowledgements

The authors acknowledge the constant encouragement, support and guidance of Prof. G K Mehta. Useful suggestions from E Krishnakumar, R Dörner and T Tonuma at the design stages of this work are acknowledged. The authors are grateful to J Chacko for precise and excellent machining of the various components of the set up and to Sunder Rao for excellent welding jobs. The concerted effort put in by the pelletron personnel and the members of the pulsing group for delivering high quality beams during the experiment is acknowledged.

References

[1] T J Gray, C L Cocke and E Justiniano, *Phys. Rev.* **A22**, 849 (1980)
[2] A Muller, B Schuch, W Groh, E Salzborn, H F Beyer, P H Mokler and R E Olson, *Phys. Rev.* **A33**, 3010 (1986)
[3] T Tonuma, H Kumagai, T Matsuo and H Tawara, *Phys. Rev.* **A40**, 6238 (1989)
[4] R Parameswaran, R L Watson, V Horvat, G Sampoll and D A Church, *Z. Phys.* **D32**, 61 (1994)
[5] C L Cocke, *Phys. Rev.* **A20**, 749 (1979)
[6] G K Mehta and A P Patro, *Nucl. Instrum. Methods* **A268**, 334 (1988)
[7] M J Singh, S K Goel, R Shanker, D O Kataria, N Madhavan, J J Das, A Tripathi, P Sugathan, D K Avasthi and A K Sinha, *Indian J. Phys.* **B69**, 181 (1995)
[8] J Ullrich, K Bethge, S Kelbch, W Schadt, H Schmidt Bocking and K E Steibing, *J. Phys.* **B19**, 437 (1986)
[9] T Tonuma, T Matsuo, H Kumagai, S H Be and H Tawara, *RIKEN Accel. Prog. Rep.* **18**, 197 (1984)
[10] D K Avasthi, Ambuj Tripathi, D Kabiraj, S Venketaramanan and S K Datta, *NSC Annual Report* **30**, 42 (1991)
[11] W C Wiley and I H Mclaren, *Rev. Sci. Instrum.* **26**, 1150 (1955)
[12] J J Das, D O Kataria, Jaipal, N Madhavan and A K Sinha, *DAE Symp. Nucl. Phys.* **B36**, 412 (1993)